STM JOURNALS

Emerging Trends in
Metabolites

Volume 1, Issue 1, 2024
January–June
DOI (Journal): 10.37591/ETM

https://journals.stmjournals.com/etm

Research ETM

# Insilico Analysis and Homology Modeling of Tetrahydroprotoberberine Oxide Involved in Berberine Biosynthesis

Kanchan Kumari[1,*]

***Abstract***

***Objective:*** *Berberine, a bioactive compound found in various plant species, exhibits diverse pharmacological properties with potential applications in pharmaceutical research. The biosynthesis of berberine involves several enzymatic steps, with (S)-tetrahydroprotoberberine oxidase playing a pivotal role. This study aimed to elucidate the structural and functional characteristics of (S)-tetrahydroprotoberberine oxidase to better understand its role in berberine biosynthesis and its potential biotechnological applications.* ***Methods:*** *Using bioinformatics tools and computational methods, the physicochemical properties, secondary structure, and molecular functions of the enzyme were analyzed. Predictions of solvent accessibility, transmembrane topology, and protein-protein interaction sites were made to gain insights into its structural organization and functional implications. Additionally, KEGG pathway analysis revealed the enzyme's involvement in metabolic pathways relevant to berberine biosynthesis and plant metabolism.* ***Results:*** *The results provided valuable insights into the (S)-tetrahydroprotoberberine oxidase enzyme, highlighting its potential as a target for biotechnological applications and pharmaceutical development. However, the study acknowledges the limitations inherent in computational predictions and emphasizes the need for experimental validation to confirm the findings.* ***Conclusion:*** *Overall, this research contributes to our understanding of (S)-tetrahydroprotoberberine oxidase and lays the groundwork for future studies aimed at exploring its biochemical properties and applications in various fields. Overall, this research contributes to our understanding of (S)-tetrahydroprotoberberine oxidase and lays the groundwork for future studies aimed at exploring its biochemical properties and applications in various fields. Future work should focus on experimental validation of the computational predictions, which will be crucial for harnessing the enzyme's full potential in pharmaceutical and biotechnological innovations.*

**Keywords:** Berberine, (S)-tetrahydroprotoberberine oxidase, THP Oxidase, *Berberis wilsoniae*, Insilico analysis

## INTRODUCTION

Nature is always a golden sign to show the prominent coexistence phenomena and provide natural products for treating human diseases [1]. Plants are a main source of natural products that hold various therapeutic properties [2]. Since ancient times, medicinal plants have been used, and they may even be considered the origin of modern medicine [2]. The term medicinal plants mean these plants have medicinal activities that can help in drug development [3]. In the Indian subcontinent, there are 17,000 species of flowering plants, and among these, only 1000 species of useful medicinal plants are reported [4]. In the future, we can harness the full potential of medicinal plants for better human health and well-being [5].

***Author for Correspondence**
Kanchan Kumari
E-mail: kkumari99704@gmail.com

[1]Student, Department of Biotechnology, Patna University, Patna, Bihar, India

Received Date: June 22, 2024
Accepted Date: June 29, 2024
Published Date: July 01, 2024

**Citation:** Kanchan Kumari. Insilico Analysis and Homology Modeling of Tetrahydroprotoberberine Oxide Involved in Berberine Biosynthesis. Emerging Trends in Metabolites. 2024; 1(1): 7–26p.

 

Medicinal plants have significant importance in various aspects of healthcare, traditional medicine, and pharmacology due to their rich source of bioactive compounds [6]. Bioactive compounds are found in various natural sources, including medicinal plants, and encompass a wide range of chemical classes, such as flavonoids, polyphenols, alkaloids, terpenoids, etc. [7]. The presence of these compounds provides multiple biological effects such as anticarcinogenic, antiallergenic, antioxidant, antimutagenic, anti-inflammatory, etc. activities that help treat non-communicable and neurodegenerative diseases [8]. Kaempferol (KPF), a flavonoid, addresses its promising effect on the central nervous system (CNS) [9]. Curcumin, resveratrol, and tea polyphenols offer therapeutic benefits owing to their antioxidant properties, modulatory role in cell signaling and display of neuroprotective effects in experimental models of CNS diseases [10]. Approximately 70–95% of people in developing countries currently use traditional medicine [11].

Alkaloids have been widely studied for their pharmacological properties and therapeutic potential [12]. The word "alkaloid" was first coined by the German chemist Carl F. W. Meissner in 1819, derived from the Al-Qali [13]. Alkaloids are a type of chemical compound that contains nitrogen and are essential to the ecology of organisms because they function as a barrier against animals and infections [14]. The alkaloids that are present in plants like caffeine, atropine, nicotine, morphine, cocaine, boldine, berberine, etc. [14, 15]. All alkaloids are basic, crystalline, odorless, bitter, and colorless; the alkaloid salts are water-soluble, and the free bases of alkaloids are soluble in organic non-polar
solvents [16].

In this paper, we focus on Berberine (BBR) alkaloid, which is a yellow-colored natural compound found in various plant families, including *Berberidaceae, Annonaceae, Menispermaceae, Ranunculaceae, Papveraceae,* etc. [17]. The BBR synthesis is indeed high in the Berberidaceae family, which is why these plants are valued in traditional medicine systems and are the focus of scientific research exploring their potential health benefits.

The *Berberis* genus, which belongs to the *Berberidaceae* family, is known to produce relatively high concentrations of BBR compared to other plants and *Berberis* species, *Berberis wilsoniae*, are recognized as significant natural sources of BBR alkaloid [18]. The chemical formula is C20H18NO4, the IUPAC name is 16,17-dimethoxy-5,7-dioxa-13-azoniapentacyclo, and the molecular weight is 336.36 g/mol of BBR [19]. Potential health effects of BBR include reducing cholesterol, controlling blood sugar levels, being antimicrobial, anti-inflammatory, antitumor, antidepressant, weight management, etc. [20] and being used to treat neurodegenerative disorders like epilepsy, Parkinson's, and Schizophrenia diseases, etc.

The overall biosynthesis of BBR starts with the two molecules of L-tyrosine molecules, i.e., dopamine and *p*-hydroxy-phenylacetaldehyde, and in the presence of norcoclaurine synthase, they are converted into (S)-norcoclaurine. Then, (S)-norcoclaurine is converted into (S)-coclaurine in the presence of SAM-dependent-O-methyl transferase enzyme. With the presence of the SAM-dependent *N*-methyl enzyme (S)-coclaurine is converted into (S)-reticuline [21], and S-reticuline is the central intermediate for the biosynthesis of BBR. Now, S-reticuline is converted into S-scoulerine with the flavin-dependent berberine bridge enzyme. Then, S-scoulerine is converted into S-tetrahydrocolumbamine with the enzyme SAM-dependent O-methyl transferase; now, S-tetrahydrocolumbamine converted into S-canadine with the help of Heme-dependent canadine synthase; and finally, S-canadine, catalyzed by tetrahydroprotoberberine oxidase (THP oxidase), is the final enzyme responsible for synthesizing BBR [22]. Modulation of THP oxidase expression or activity can potentially alter the levels of BBR and related alkaloids in plant tissues [23].

So, using bioinformatics tools, we analyzed the functional and structural characteristics of THP

 

Oxidase.

## METHODOLOGY

### Retrieval of Sequence

Using NCBI (National Center for Biotechnology Information) (https://www.ncbi.nlm.nih.gov/), we retrieved the FASTA sequence of (S)-tetrahydroprotoberberine oxidase of *Berberis wilsoniae,* and its accession number was ADY15026.1, and this sequence was highly similar to tetrahydroberberine oxide.

### Analysis of Physicochemical Properties

To investigate valuable parameters of proteins like amino acid residues, molecular weight, pI, instability index, grand average of hydropathicity (GRAVY), etc. using different bioinformatics tools, i.e., ProtParam (https://web.expasy.org/protparam/), Pepstats (https://www.ebi.ac.uk/jdispatcher/seqstats/emboss_pepstats), and PepInfo (https://www.ebi.ac.uk/jdispatcher/seqstats/emboss_pepinfo).

### Functional Characterization

SOSUI (https://harrier.nagahama-i-bio.ac.jp/sosui/mobile/) is a bioinformatics tool that is used to predict whether a given protein sequence is soluble or has transmembrane regions. An amphiphilic list of amino acid sequences was produced to enhance the approach for transmembrane helix production.

### Prediction of Secondary Structure of Protein

Self-optimized prediction method with alignment (SOPMA) (https://npsa-prabi.ibcp.fr/cgi-bin/secpred_sopma.pl) is commonly used for predicting the secondary structure of proteins, including alpha helix, beta sheet, turns, etc.

### 3D Model Building

The SWISS model (https://swissmodel.expasy.org/) is a widely used tool for protein 3D structure modeling because it aligns the target sequence with known protein structures, which helps generate the Ramachandran plot. This plot helps in assessing the quality and reliability of protein structures.

### Structure Validation

To check the protein's quality and accuracy using two bioinformatics tools, i.e., MolProbity (http://molprobity.manchester.ac.uk/) and ERRAT (https://www.doe-mbi.ucla.edu/errat/). MolProbity helps to check steric clashes, improper bond lengths and angles, and other geometric irregularities in the protein model, whereas ERRAT focuses on the agreement between the observed and expected distributions of non-bonded atom-atom interactions.

### Analysis of Biological Process

The search tool for the retrieval of interacting genes/proteins (STRING) (http://string-db.org) integrates all data from various sources, like experimental studies, computational predictions, and text mining, to predict and annotate protein-protein interactions (PPI), which can infer potential functional relationships between proteins involved in biological processes [24].

### Identification of Transmembrane topology

Phobius (https://www.ebi.ac.uk/jdispatcher/pfa/phobius) is a well-known bioinformatics tool used for predicting transmembrane topology, which plays a crucial role in various cellular processes, and signal peptides, which aid in the identification of proteins targeted for secretion or membrane insertion.

### Identification of Protein Function

The function of a protein refers to its specific role or activity within a biological system. ProFunc (https://www.ebi.ac.uk/thornton-srv/databases/Profunc) and next-generation sequence-analysis toolkit (NeST) are two tools that help identify the functions of proteins. Profunc incorporates information

 

from protein structure prediction methods to enhance accuracy, whereas the NeST tool (https://nest-simulator.org/) is valuable because it accurately predicts protein function by integrating diverse sequence and structure-based features using machine learning algorithms.

**Identification of Motifs and Domains**

Motifs and domains are crucial structural and functional elements within proteins because they serve as recognizable building blocks that indicate specific functions, such as enzymatic activity or binding sites. LEGO-CSM (https://biosig.lab.uq.edu.au/lego_csm/predict), InterProScan (https://www.ebi.ac.uk/jdispatcher/pfa/iprscan5/summary?jobId=iprscan5-I20240407-114317-0933-85329267-p1m) and MOTIF search (https://www.genome.jp/tools/motif/) are three powerful tools that help identify motifs and domains.

**Predict Subcellular Localization**

Subcellular localization refers to the specific location within a cell where a protein is predominantly located or functions, which helps elucidate biological processes, identify potential drug targets, etc., and CELLO and plant-mPloc are two tools that accurately predict subcellular localization.

**RESULTS**

**Retrieval FASTA sequence**

The retrieval of the FASTA sequence of (S)-tetrahydroprotoberberine oxidase (STOX) (Figure.1), which is responsible for berberine synthesis in *Berberis wilsoniae,* from the NCBI database. The identical protein sequence of THP oxidase is tetrahydroberberine oxide which has possibly the same enzymatic activity (Figure 2).

```
>ADY15026.1 (S)-tetrahydroprotoberberine oxidase [Berberis wilsoniae]
MSKMASSIFATFSLLSSLLPTSLASSDANYEDFLQCLDLYSQNSIPVYTRNTSSYTSILESTIKNLVFLS
PTTPKPNFIVTPMQESHVQTSVICCRMHGLQMRIRSGGHDFEGLSYVSNVPFVVLDLIHLKTINVDIEEN
SAWVQTGATIGELYYRIAEKVGVHAFPAGLCPTVGVGGHISGAGYGVLMRKYGVSADHVIDARIVNVDGE
ILDRESMGEDLFWAIRGGGGASFGVILAWKIRLVPVPPTVTIFIVPKTLEEGATALLHKWQFIGDNVHED
LFIGLSMRSVIISPKGDKTILVSFIGLFLGGSDKLVQHMEQSFPELGVKPHDCIEMSWIKSTVVFGVFSN
DASLSVLLDRKNPFPPKSYHKVKSDYVTEPLPISVLEGICHRFLKNGVNKAEIIMSPYGGRMNEISESEI
AFPHRKGNLYKINYIAEWEEAGSMENHLSWIRELYRYMTPYVSKSPRSSYLNFKDIDLGQTKNGTATYSQ
AKAWGSKYFKNNFKRLMQVKTKVDPNNFFCNEQGIPPFSS
```

**Figure 1.** FASTA sequence of ADY15026.1

```
>sp|F1BVB6.1|STOX_BERWI RecName: Full=Tetrahydroberberine oxidase; Short=THB oxidase;
AltName: Full=(S)-tetrahydroprotoberberine oxidase; Short=BwSTOX; Flags: Precursor
MSKMASSIFATFSLLSSLLPTSLASSDANYEDFLQCLDLYSQNSIPVYTRNTSSYTSILESTIKNLVFLS
PTTPKPNFIVTPMQESHVQTSVICCRMHGLQMRIRSGGHDFEGLSYVSNVPFVVLDLIHLKTINVDIEEN
SAWVQTGATIGELYYRIAEKVGVHAFPAGLCPTVGVGGHISGAGYGVLMRKYGVSADHVIDARIVNVDGE
ILDRESMGEDLFWAIRGGGGASFGVILAWKIRLVPVPPTVTIFIVPKTLEEGATALLHKWQFIGDNVHED
LFIGLSMRSVIISPKGDKTILVSFIGLFLGGSDKLVQHMEQSFPELGVKPHDCIEMSWIKSTVVFGVFSN
DASLSVLLDRKNPFPPKSYHKVKSDYVTEPLPISVLEGICHRFLKNGVNKAEIIMSPYGGRMNEISESEI
AFPHRKGNLYKINYIAEWEEAGSMENHLSWIRELYRYMTPYVSKSPRSSYLNFKDIDLGQTKNGTATYSQ
AKAWGSKYFKNNFKRLMQVKTKVDPNNFFCNEQGIPPFSS
```

**Figure 2.** Identical protein of THP oxidase.

**Physicochemical Properties**:

ADY15026.1 comprises 530 amino acid residues, has a hydrophilic nature, and its molecular

 

weight is 58989.77. Due to its instability index of 36.41 and aliphatic index of 89.70, that indicates the selected protein is stable. This protein is hydrophilic because its GRAVY number is negative, i.e., -0.059. Table 1 shows each of this protein's (ADY15026.1) physicochemical characteristics.

**Table 1.** Physicochemical characteristics of ADY15026.1.

| | |
|---|---|
| No. of amino acids | 530 |
| Molecular weight | 58989.77 |
| Theoretical pI | 6.95 |
| Total number of negatively charged residues (Asp + Glu) | 51 |
| Total number of positively charged residues (Arg + Lys) | 50 |
| Formula | $C_{2670}H_{4142}N_{694}O_{770}S_{22}$ |
| Total number of atoms | 8298 |
| Instability index | 36.41 (This classifies the protein as stable) |
| Aliphatic index | 89.70 |
| GRAVY | -0.059 |
| Extinction coefficients | 73800 (Abs 0.1% (=1 g/l), 1.251, assuming all Cys residues are reduced)<br>74175 (Abs 0.1% (-1 g/l), 1.257, assuming all pairs of Cys residues form cystines) |
| Estimated half-life | 30 hours |
| Total length of protein sequence | 530 AA |
| Average of hydrophobicity | -0.058679 |

## Functional Characterization

Using SOSUI, we also observed the length of the protein sequence, an average hydrophobicity of 0.058679 (Table 2), and a C-terminal signal peptide that indicates it is located at the end of the protein; it guides the protein to its destination within the cell or outside the cell for ensuring proper secretion or localization; it may be involved in targeting proteins to specific organelles or directing them for secretion.

**Table 2.** Hydrophobicity is calculated by SOSUI.

**This amino acid sequence has signal peptide.**

| No. | N terminal | transmembrane region | C terminal | type | length |
|---|---|---|---|---|---|
| 0 | 1 | MSKMASSIFATFSLLSSLLPTSLAS | 25 | SignalPeptide | 25 |

## Protein Sequence Analysis & Protein Info

PepStats and PepInfo are the two online tools that provide detailed knowledge of selected proteins. PepStats also provide physicochemical properties like ProtParam, additionally, they provide the charge of the protein, i.e., 6.5 (Tables 3 and 4), which implies the selected protein sequence was neutral, whereas PepInfo gives a hydropathy plot (Figure 3).

**Table 3.** Result by PepStats.

| | |
|---|---|
| Molecular weight | 58989.77 |
| Residues | 530 |
| Average residue Weight | 111.301 |
| Charge | 6.5 |
| Isoelectric point | 7.3421 |
| A280 molar extinction coefficients | 73800 (reduced) 74175 (cystine bridges) |
| A280 extinction coefficients 1mg/ml | 1.251 (reduced) 1.257 (cystine bridges) |
| Improbability of expression in inclusion bodies | 0.839 |

**Table 4.** Statistics of amino acid residues provided by the Pepstats server.

| Properties | Residues | Number | Mole (%) |
|---|---|---|---|

 

| | | | |
|---|---|---|---|
| Tiny | (A+C+G+S+T) | 152 | 28.679 |
| Small | (A+B+C+D+G+N+P+S+T+V) | 268 | 50.566 |
| Aliphatic | (A+I+L+V) | 151 | 28.491 |
| Aromatic | (F+H+W+Y) | 70 | 13.208 |
| Non-polar | (A+C+F+G+I+L+M+P+V+W+Y) | 297 | 56.038 |
| Polar | (D+E+H+K+N+Q+R+S+T+Z) | 233 | 43.962 |
| Charged | (B+D+E+H+K+R+Z) | 116 | 21.887 |
| Basic | (H+K+R) | 65 | 12.264 |
| Acidic | (B+D+E+Z) | 51 | 9.623 |

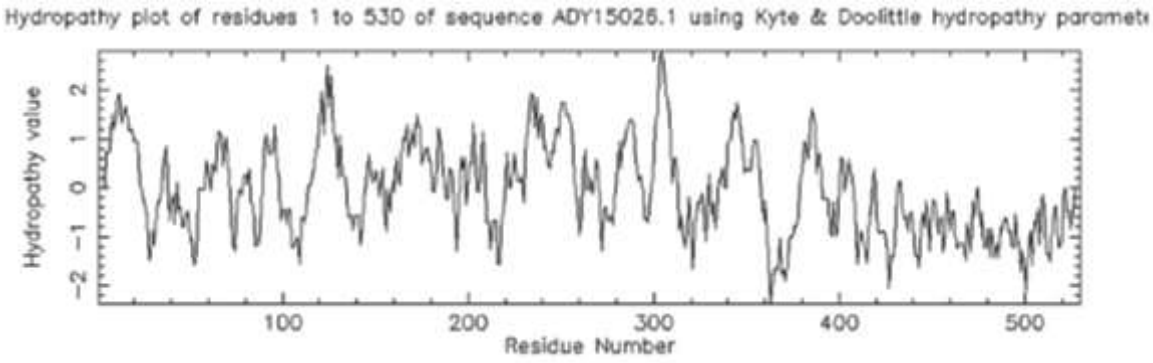


**Figure 3.** Hydropathy plot by Pepinfo server.

**Secondary Structure Prediction**

The secondary structure prediction results obtained from SOPMA for the protein tetrahydroprotoberberine oxide reveal a diverse distribution of structural elements within its sequence. In Figures 4 and 5, the different colors represent the different structures, which means the blue color represents the helical structure, the red color represents beta-strand conformation, the green color represents each turn, and the pink color represents the coils, which means that parts do not form regularly secondary structures, often connecting helices and strands in the protein sequence. Table 5 reveals a diverse distribution of structural elements within its sequence. The analysis indicates the presence of 168 residues forming alpha helices, with 31 residues adopting a helical conformation (H) and the remainder having a helical propensity (h). Additionally, 110 residues are predicted to form extended strands, with 20 residues adopting an extended conformation (E) and the rest displaying an extended propensity (e). Notably, the majority of residues, totaling 252, are anticipated to be in a random coil conformation, with 47 residues in a coil conformation (C).

 

```
        10        20        30        40        50        60        70
         |         |         |         |         |         |         |
MSKMASSIFATFSLLSSLLPTSLASSDANYEDFLQCLDLYSQNSIPVYTRNTSSYTSILESTIKNLVFLS
hhhhhhhhhhhhhhhhhhccchhhhccccchhhhhhhhhcccccceeeecccccchhhhhhhhhhhheecc
PTTPKPNFIVTPMQESHVQTSVICCRMHGLQMRIRSGGHDFEGLSYVSNVPFVVLDLIHLKTINVDIEEN
cccccceeeeccccchhhhhhhhhhcctteeeeeettccceeeeeeccccceeeeehhhhceeeeecccc
SAWVQTGATIGELYYRIAEKVGVHAFPAGLCPTVGVGGHISGAGYGVLMRKYGVSADHVIDARIVNVDGE
heeehttcchhhhhhhhhccccceeccttccceeeeeeeecccccchhhhhhttcccchhhhheeectttc
ILDRESMGEDLFWAIRGGGGASFGVILAWKIRLVPVPPTVTIFIVPKTLEEGATALLHKWQFIGDNVHED
eechtcccchheeeeecttcccceeeeeeeeeeeecccccceeeeeecccccttthhhhhhhhhhhcccccth
LFIGLSMRSVIISPKGDKTILVSFIGLFLGGSDKLVQHMEQSFPELGVKPHDCIEMSWIKSTVVFGVFSN
heeeeeeeecccccccccceeeeehheeeccchhhhhhhhhtcccccccccchhhhhhhhhheeeccccc
DASLSVLLDRKNPFPPKSYHKVKSDYVTEPLPISVLEGICHRFLKNGVNKAEIIMSPYGGRMNEISESEI
ccccchheehhhccccccceecccccecccccchhhhhhhhhhhhhhcttccceeeeccttcccccccccc
AFPHRKGNLYKINYIAEWEEAGSMENHLSWIRELYRYMTPYVSKSPRSSYLNFKDIDLGQTKNGTATYSQ
ccccttceeeeeeeeecccccchhhhhhhhhhhhhhhhhhhcccctteeeeeeeeeecccccccchhh
AKAWGSKYFKNNFKRLMQVKTKVDPNNFFCNEQGIPPFSS
hhhhtchhhhcchhhhhhhhccccttceecccccccccc
```

**Figure 4.** FASTA characterization by the SOPMA server.

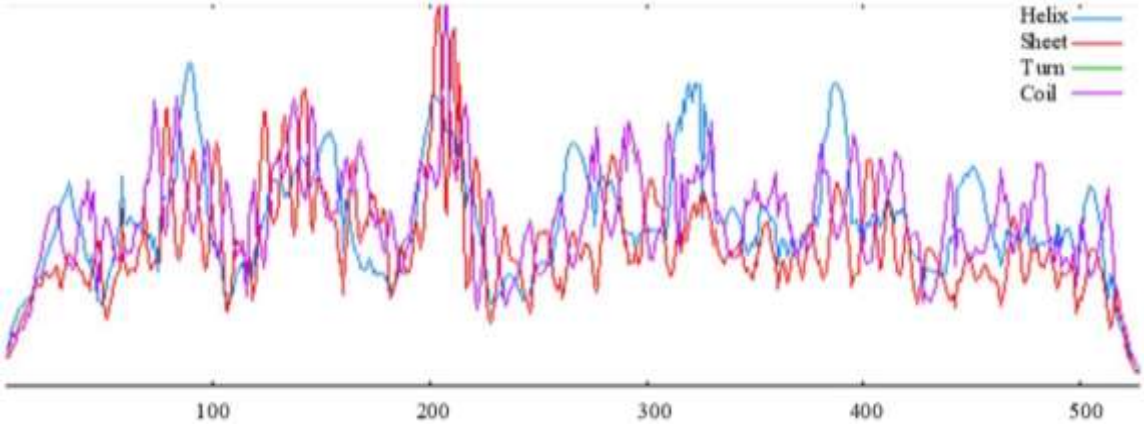


**Figure 5.** Secondary structure characteristics of SOPMA.

**Table 5.** Secondary structure prediction by SOPMA.

| | | |
|---|---|---|
| Alpha helix (Hh) | 168 | 31 |
| 310 helix (Gg) | 0 | 0 |
| Pi helix (Ii) | 0 | 0 |
| Beta bridge (Bb) | 0 | 0 |
| Extended strand (Ee) | 110 | 20 |
| Beta turn (Tt) | 0 | 0 |
| Bend region (Ss) | 0 | 0 |
| Random coil (Cc) | 252 | 47 |
| Ambiguous states (?) | 0 | 0 |
| Other states | 0 | 0 |

**Model Building and Evaluation**

The results obtained from the SWISS model indicate that FIBVB6.1. A tetrahydroberberine oxidase serves as the most suitable template for modeling the 3D structure of the protein ADY15026.1 (Figure 6). Leveraging this template allows for the generation of a reliable structural model for the protein of interest. The GMQE (global model quality estimation) score, which assesses the overall quality of the

 

predicted model, is notably high at 0.93. This score reflects confidence in the structural accuracy of the model, considering factors such as template suitability, alignment quality, and model coverage. Figure 7 displays the protein's three-dimensional structure, whereas Figure 8 uses the SWISS model to illustrate the protein's Ramachandran plot.

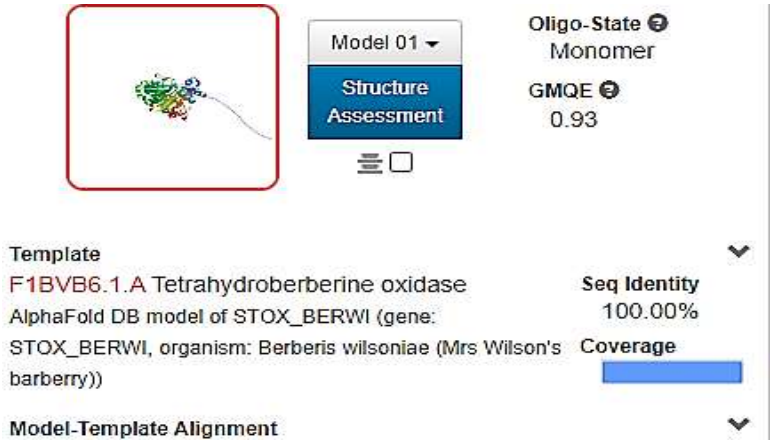


**Figure 6.** F1BVB6.1. A template for modeling.

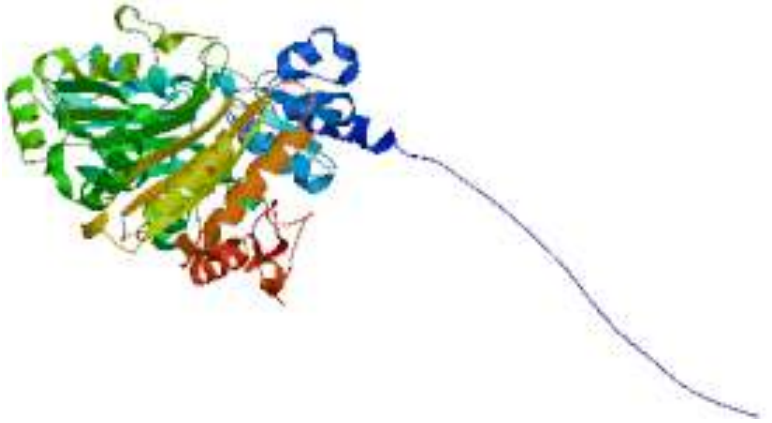

**Figure 7.** 3D structure of protein.

 

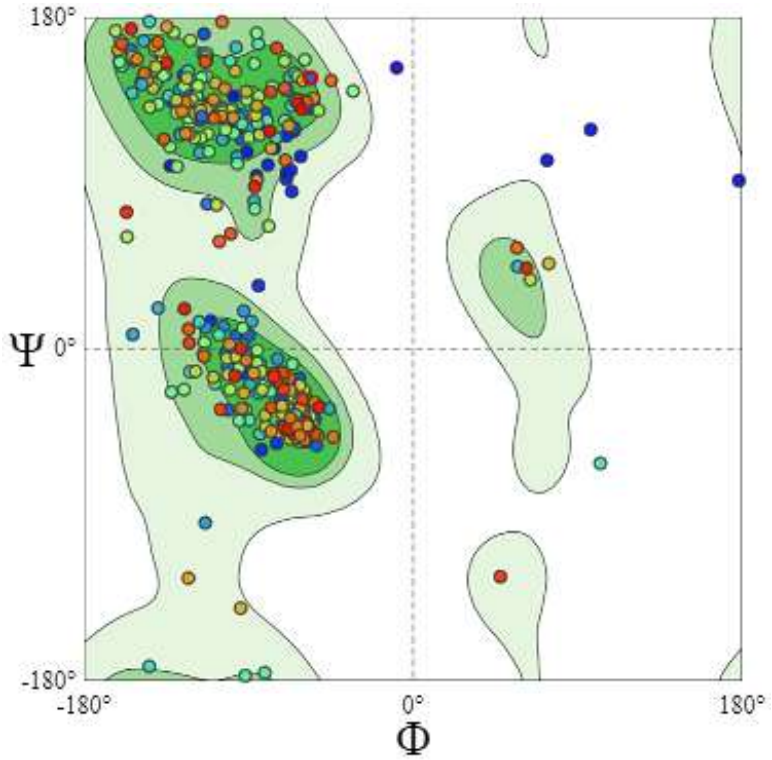


**Figure 8.** Ramachandran plot by SWISS model.

**Structure Validation**

The results obtained from MolProbity and ERRAT provide valuable insights into the structural quality and accuracy of the protein model. MolProbity scores a remarkable 1.00, indicating excellent geometry and minimal steric clashes within the protein structure (Table 6). Similarly, ERRAT assigns a structure quality factor of 95.400 to ADY15026.1, indicating a high-quality protein structure with very few errors (Figure 9).

**Table 6.** MolProbity result.

| | |
|---|---|
| MolProbity score | 1.00 |
| Clash score | 0.36 |
| Ramachandran favoured | 94.70% |
| Ramachandran outliers | 1.14% |
| A423 PRO, A278 HIS, A6 SER, A5 ALA, A183 ALA, A2 SER | |
| Rotamer outliers | 0.43% |
| A15 LEU, A23 LEU | |
| C-beta deviations | 4 |
| A6 SER, A4 MET, A181 SER, A400 LYS | |
| Bad bonds | 0 / 4262 |
| Bad angles | 38 / 5781 |
| (A2 SER-A3 LYS), (A1 MET-A2 SER), A477 ASP, (A3 LYS-A4 MET), (A459 THR-A460 PRO), A364 PHE, A68 PHE, (A521 ASN-A522 GLU), A6 SER, A276 ASN, (A45 ILE-A46 PRO), A331 HIS, A208 ASP, (A379 GLU-A380 PRO), A198 HIS, A278 HIS, A183 ALA, A391 HIS, A164 HIS, A239 TRP, A4 MET, A87 HIS, A268 HIS, A494 TRP, A129 HIS, A98 HIS, A179 HIS, (A525 ILE-A526 PRO), (A120 VAL-A121 PRO), (A166 PHE-A167 PRO), (A182 GLY-A183 ALA), A424 HIS, A195 SER, A318 HIS | |
| Cis non-proline | 1 / 501 |
| (A2 SER-A3 LYS) | |
| Cis prolines | 2 / 28 |
| (A364 PHE-A365 PRO), (A465 SER-A466 PRO) | |
| Twisted non-proline | 2 / 501 |

 

(A3 LYS-A4 MET), (A5 ALA-A6 SER)

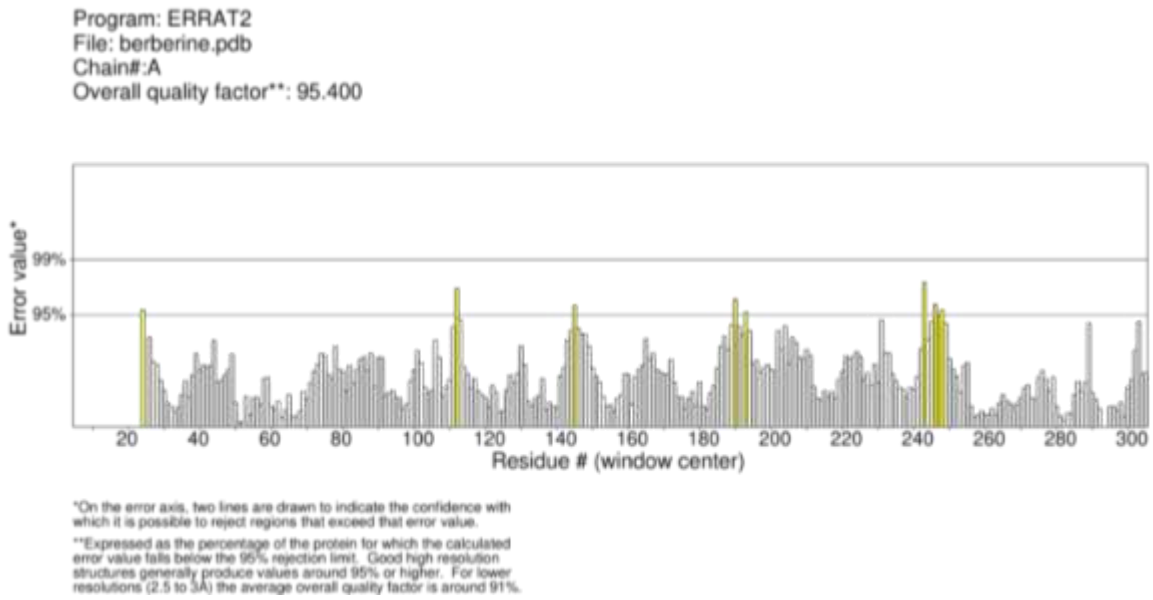


**Figure 9.** ERRAT result

**PDBsum**

PDBsum provides information on a protein structure as deposited in the Protein Data Bank (PDB), like structure summary, protein chains, structure quality, 3D visualization, functional sites, interactions, secondary structure, sequence features, etc. (Table 7).

**Table 7.** PDBsum result

| | PDB code | Model | Length | %-tage identity | A.A. overlap | Z-score | Ligands | Protein name |
|---|---|---|---|---|---|---|---|---|
| 1. | 8ate(A) | X-ray 1.92Å | 502 | 53.6% | 504 | 2514.9 | FAD, NAG, GOL, PEG. | Galacturonic acid oxidase from citrus sinensis |
| 2. | 3vte(A) | X-ray 2.75Å | 502 | 50.5% | 501 | 2304.3 | NAG, FAD. | Crystal structure of tetrahydrocannabinolic acid synthase from cannabis sativa |
| 3. | 5d79(A) | X-ray 1.85Å | 498 | 48.6% | 504 | 2206.6 | PO4, FAD. | Structure of bbe-like #28 from arabidopsis thaliana |
| 4. | 4ud8(A) | X-ray 2.09Å | 500 | 51.5% | 505 | 2184.8 | NAG-NAG, FAD, NAG, PE5. | Atbbe15 |
| 5. | 7e2v(A) | X-ray 2.94Å | 500 | 48.0% | 504 | 2131.8 | FAD, NAG. | Crystal structure of mada-3 |
| 6. | 6jqh(A) | X-ray 2.30Å | 504 | 47.5% | 510 | 2131.7 | FAD. | Crystal structure of mada |
| 7. | 3d2h(A) | X-ray 1.65Å | 498 | 38.8% | 510 | 1403.6 | NAG-NAG-MAN-MAN-MAN-MAN, NAG, FAD, FSH. | Structure of berberine bridge enzyme from eschscholzia californica, monoclinic crystal form |

 

| | | | | | | | | |
|---|---|---|---|---|---|---|---|---|
| 8. | 3d2j(A) | X-ray 2.05Å | 502 | 38.8% | 510 | 1403.5 | NAG-NAG-MAN, NAG, FAD. | Structure of berberine bridge enzyme from eschscholzia californica, tetragonal crystal form |
| 9. | 3fw9(A) | X-ray 1.49Å | 495 | 38.9% | 509 | 1402.4 | NAG-NAG-MAN, FAD, SLX, NAG. | Structure of berberine bridge enzyme in complex with (s)-scoulerine |
| 10. | 3gsy(A) | X-ray 1.63Å | 495 | 38.9% | 509 | 1402.4 | NAG-NAG-BMA, FAD, DEH, NAG. | Structure of berberine bridge enzyme in complex with dehydroscoulerine |

**Protein-Protein Interaction Network**

A protein-protein interaction (PPI) network is a graphical representation of interactions between proteins within a biological system. The network of interactions between proteins is based on experimental evidence and computational predictions. Proteins are represented as nodes, and interactions between proteins are represented as edges in the network (Figure 10).


**Figure 10.** Protein-protein interaction by STRINGA

**INTERPro**

Comprehensive information about protein sequences (ADY15026.1), including domain architectures, functional motifs, and other structural features (Figure 11).

 

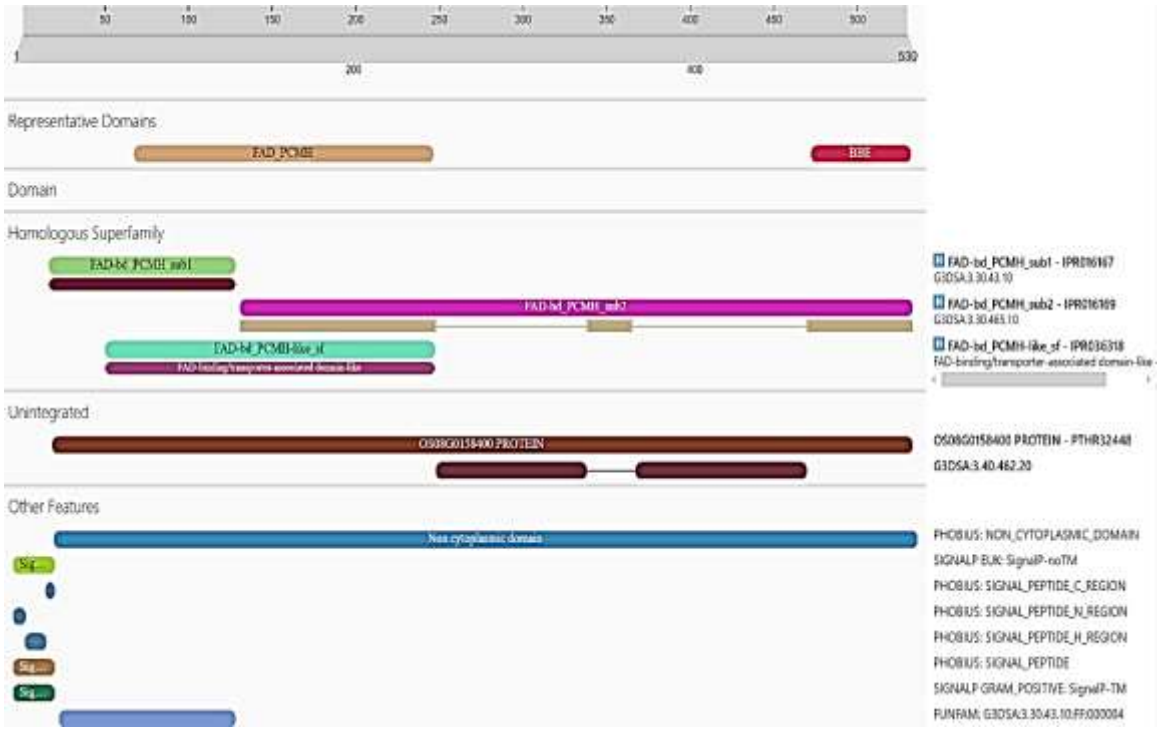


**Figure 11.** Protein hierarchy by InterPro

**PHOBIUS**

In Figure 12, the presence of a signal sequence (SIGNAL) from amino acid positions 1 to 24 suggests that the protein likely undergoes cotranslational translocation, meaning it is targeted to the secretory pathway for secretion or membrane integration. The protein sequence is divided into three distinct regions: (a) N-REGION (1–7): This region typically corresponds to the N-terminal signal sequence, responsible for directing the nascent protein to the endoplasmic reticulum (ER) for further processing. (b) H-REGION (8-19): This region may represent a hydrophobic stretch involved in the signal sequence cleavage process or membrane integration and (c) C-REGION (20–24): This region is likely part of the signal sequence and may play a role in signal peptide cleavage and the TOPO_DOM annotation indicates that the majority of the protein (from amino acid position 25 to 530) is non-cytoplasmic, suggesting that it is localized outside the cell. This localization implies that the protein may be secreted from the cell or integrated into cellular membranes.

ID ADY15026.1
FT SIGNAL 1 24
FT REGION 1 7 N-REGION.
FT REGION 8 19 H-REGION.
FT REGION 20 24 C-REGION.
FT TOPO_DOM 25 530 NON-CYTOPLASMIC.

**Figure 12.** Phobius result.

**Identification of Protein Function**

In Table 8, all information on protein residues, such as the cleft, depth of the cleft, solvent accessibility, Ramchandran region, residue range, etc., is compiled by the NeST tool.

**Table 8.** NeST result.

| Nest | Score | Residue range | View in RasMol | Residue | Ramachandran region | Solvent accessibility | Cleft | Depth in cleft | Residue conservation |
|---|---|---|---|---|---|---|---|---|---|

 

| | | | | | | | | | |
|---|---|---|---|---|---|---|---|---|---|
| 1. | 6.00 | Gly107(A)-His109(A) |  | Gly107(A) | RIGHT | 2.72% |  | - | 1.00 |
| | | | | Gly108(A) | LEFT | 3.01% |  | - | 1.00 |
| | | | | His109(A) | - | 3.40% |  | - | 1.00 |
| 2. | 4.47 | Glu112(A)-Ser115(A) |  | Glu112(A) | RIGHT | 0.00% | - | - | 1.00 |
| | | | | Gly113(A) | LEFT | 0.00% | - | - | 1.00 |
| | | | | Leu114(A) | RIGHT | 0.00% | - | - | 0.86 |
| | | | | Ser115(A) | RIGHT | 0.01% |  | - | 1.00 |
| 3. | 4.23 | Val347(A)-Ser349(A) |  | Val347(A) | RIGHT | 0.00% | - | - | 0.53 |
| | | | | Phe348(A) | LEFT | 0.00% | - | - | 0.63 |
| | | | | Ser349(A) | - | 0.02% |  | - | 0.52 |
| 4. | 4.00 | Gly227(A)-Gly229(A) |  | Gly227(A) | LEFT | 0.00% | - | - | 1.00 |
| | | | | Gly228(A) | RIGHT | 0.00% | - | - | 1.00 |
| | | | | Gly229(A) | - | 0.00% |  | 30.67 | 1.00 |
| 5. | 3.53 | Leu326(A)-Val328(A) |  | Leu326(A) | RIGHT | 0.00% | - | - | 0.75 |
| | | | | Gly327(A) | LEFT | 0.29% | - | - | 1.00 |
| | | | | Val328(A) | - | 1.96% | - | - | 0.83 |
| 6. | 3.22 | Lys295(A)-Asp297(A) |  | Lys295(A) | RIGHT | 0.00% | - | - | 0.47 |
| | | | | Gly296(A) | LEFT | 0.04% | - | - | 0.64 |
| | | | | Asp297(A) | - | 0.04% | - | - | 0.56 |
| 7. | 2.74 | Glu261(A)-Thr264(A) |  | Glu261(A) | RIGHT | 0.00% | - | - | 0.71 |
| | | | | Gly262(A) | LEFT | 1.08% | - | - | 0.87 |
| | | | | Ala263(A) | RIGHT | 0.00% | - | - | 0.91 |
| | | | | Thr264(A) | RIGHT | 0.01% | - | - | 0.49 |
| 8. | 2.51 | His98(A)-Leu100(A) |  | His98(A) | RIGHT | 0.00% | - | - | 0.85 |
| | | | | Gly99(A) | LEFT | 1.02% | 4 | - | 0.78 |
| | | | | Leu100(A) | - | 0.00% | 6 | 4.54 | 0.90 |
| 9. | 2.45 | Asn483(A)-Thr485(A) |  | Asn483(A) | RIGHT | 1.19% | 3 | 9.02 | 0.70 |
| | | | | Gly484(A) | LEFT | 0.00% | - | - | 0.89 |
| | | | | Thr485(A) | - | 0.00% | - | - | 0.78 |
| 10. | 1.84 | Asn516(A)-Phe519(A) |  | Asn516(A) | RIGHT | 0.00% | 8 | - | 0.64 |

 

| | | | | | | | | | |
|---|---|---|---|---|---|---|---|---|---|
| | | | | Asn517(A) | LEFT | 0.00% | - | - | 0.73 |
| | | | | Phe518(A) | RIGHT | 0.00% | 4 | 4.74 | 1.00 |
| | | | | Phe519(A) | - | 0.00% | - | - | 1.00 |
| 11. | 0.79 | Asp208(A)-Glu210(A) | | Asp208(A) | RIGHT | 0.00% | - | - | 0.72 |
| | | | | Gly209(A) | LEFT | 0.00% | - | - | 1.00 |
| | | | | Glu210(A) | - | 0.00% | - | - | 0.65 |
| 12. | 0.68 | Glu139(A)-Ser141(A) | | Glu139(A) | RIGHT | 0.00% | - | - | 0.64 |
| | | | | Asn140(A) | LEFT | 0.00% | - | - | 0.68 |
| | | | | Ser141(A) | - | 0.00% | - | - | 0.73 |

**Identification of Motifs and Domains**

For the identification of the motifs and domains, we used 3 software tools, i.e., MOTIF Search, LEGO-CSM, and InterProScan. The presence of conserved sequence patterns such as FAD_bindin_4, BBE, Sulfotransfer_5, and PAH (Figure 13) within the ADY15026.1 protein sequence, identified using MOTIF Search, can provide insights into its potential biological functions. These motifs are associated with specific protein domains or functional sites, which can suggest roles in processes such as binding to FAD (flavin adenine dinucleotide), enzymatic activities related to BBE (berberine bridge enzyme), sulfotransferase functions, and phenylalanine hydroxylase (PAH) activity.

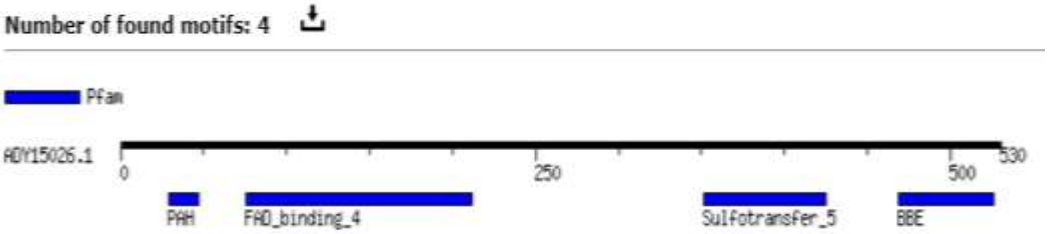


**Pfam** (4 motifs)

| Pfam | Position(Independent E-value) | | Description |
|---|---|---|---|
| FAD_binding_4 | 76..212(1.3e-24) | Detail | PF01565, FAD binding domain |
| BBE | 469..526(1.5e-19) | Detail | PF08031, Berberine and berberine like |
| Sulfotransfer_5 | 351..425(0.033) | Detail | PF19798, Sulfotransferase domain |
| PAH | 29..47(0.21) | Detail | PF02671, Paired amphipathic helix repeat |

**Figure 13.** Motifs of protein by MOTIF Search.

The localization of the ADY15026.1 protein predominantly on the extracellular side of the membrane suggests that it may be involved in processes that occur outside the cell, such as cell signaling, adhesion, or interactions with the extracellular environment (Figure 14).

Additionally, the classification of the enzyme associated with ADY15026.1 as belonging to the oxidoreductases class indicates that it likely catalyzes oxidation-reduction reactions, where electrons are transferred between molecules that play crucial roles in various metabolic pathways, including energy production, detoxification, and biosynthesis.

 

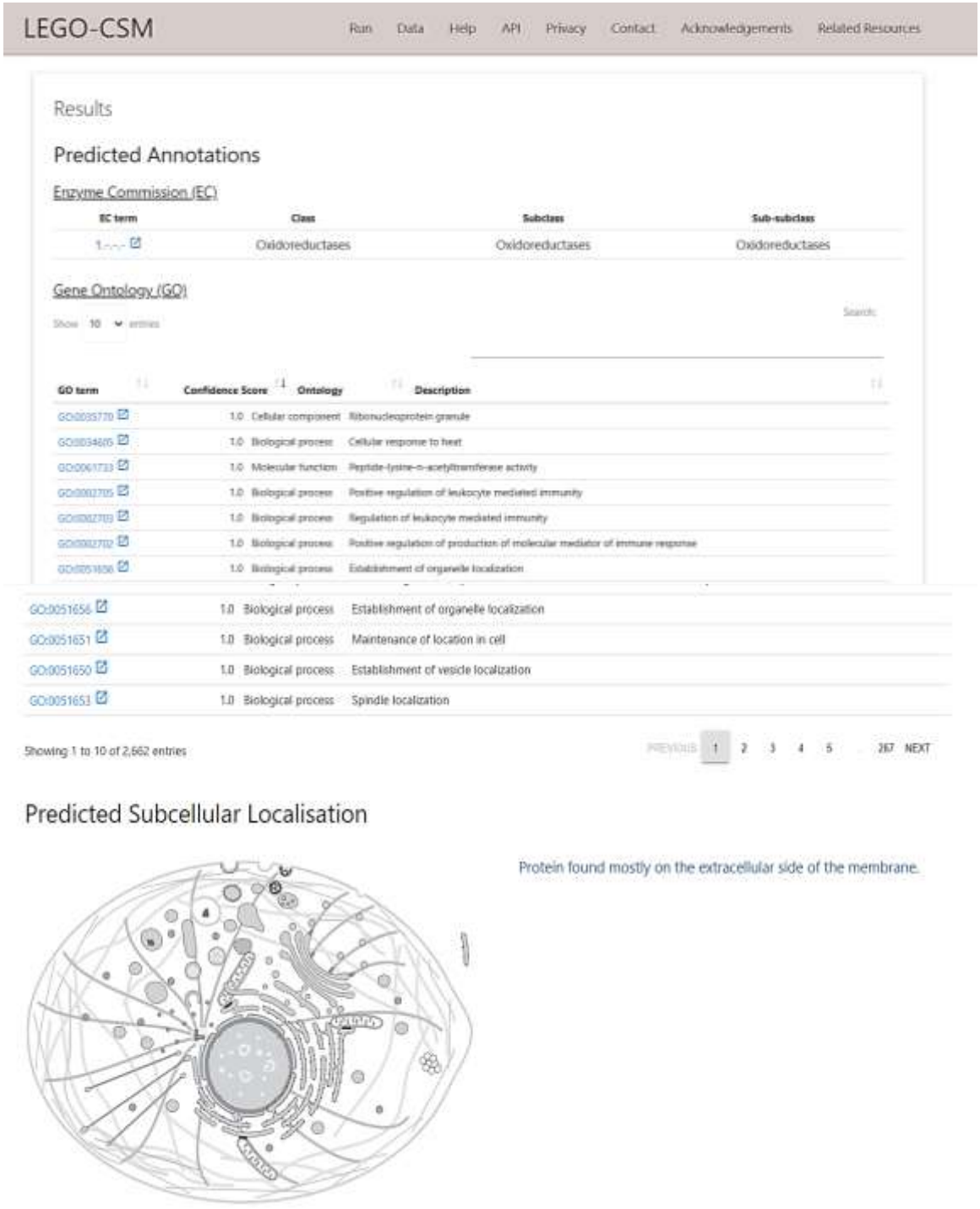


**Figure 14.** LEGO-CSM result

InterProScan integrates various software tools and databases to predict and annotate functional domains, sites, and motifs within a protein sequence, compared to using individual tools separately. By utilizing InterProScan, we gain valuable insights into the structural and functional characteristics of proteins, including the identification of conserved domains, protein families, motifs, and functional sites (Figure 15).

 


**Figure 15.** InterProScan result

**Predict Protein**

Predict-protein analysis offers significant insights into the structural features, evolutionary stability, and functional interactions of S-tetrahydroprotoberberine oxidase, enhancing our understanding of its role in berberine production. In Table 9, the predicted secondary structure of the protein includes strands, helices, and other structural elements. The protein's accessibility to solvent molecules is categorized into two phases: exposed and buried, the presence of a signal peptide indicates that the protein may undergo post-translational modification or trafficking to specific cellular compartments. It consists of 530 amino acid residues, and 70 related proteins suggest evolutionary conservation across different species or protein families. Providing information about its overall size and complexity, identification of protein, and presence of 31 matched PDB structures indicates that experimental structures similar to S-tetrahydro protoberberine oxidase have been reported.

**Table 9.** Predicted features by predict protein.

| | |
|---|---|
| Secondary structure | Strand, helix, other |
| Solvent accessibility | Exposed, buried |
| Topology | Signal peptide |
| Sequence length | 530 |
| Number of aligned proteins | 70 |
| Number of matched PDB structures | 31 |

**InterProSurf**

The results obtained from the InterProSurf tool provide detailed insights into the surface properties of the protein complex, particularly focusing on solvent accessibility, hydrophobicity, and electrostatic potential. As a result, we found the probe radius of 1.400 Å indicates the size of the probe used to calculate the accessible surface area of the protein complex; the calculated polar area/energy is 8794.05, suggesting a significant portion of the protein surface is polar, allowing interactions with water molecules or other polar substances. With a value of 14598.80, the apolar area/energy indicates a substantial hydrophobic surface area, which may facilitate interactions with other hydrophobic molecules or regions. The total area/energy is 23392.85, reflecting the combined polar and apolar characteristics of the protein surface. With 2202 surface atoms, it suggests a relatively large surface area available for interactions with other molecules, and there are 1954 buried atoms, indicating the presence of a compact core within the protein complex. The Table 10 given below show area calculation for protein complex.

 

**Table 10.** Accessible Surface Area Calculation for Berberine Protein Complex.

| Probe radius: 1.400 | POLAR area/energy = 8794.05 | APOLAR area/energy = 14598.80 | Total area/energy = 23392.85 | Number of surface atoms = 2202 | Number of buried atoms = 1954 |
|---|---|---|---|---|---|

**Predict Subcellular Localization**

According to the CELLO tool, we found the presence of this protein (ADY15026.1) in different localizations and the most reliable location is the plasma membrane (Figure 16), and according to the plant m-loc, this protein (ADY15026.1) is present in the cytoplasm (Figure 17).

**CELLO RESULTS**

SeqID: ADY15026.1 (S)-tetrahydroprotoberberine oxidase [Berberis wilsoniae]

Analysis Report:

| SVM | LOCALIZATION | RELIABILITY |
|---|---|---|
| Amino Acid Comp. | PlasmaMembrane | 0.876 |
| N-peptide Comp. | PlasmaMembrane | 0.694 |
| Partitioned seq. Comp. | Chloroplast | 0.407 |
| Physico-chemical Comp. | PlasmaMembrane | 0.685 |
| Neighboring seq. Comp. | PlasmaMembrane | 0.679 |

CELLO Prediction:

| | | |
|---|---|---|
| | PlasmaMembrane | 3.116 * |
| | Chloroplast | 0.721 |
| | Cytoplasmic | 0.294 |
| | Mitochondrial | 0.215 |
| | Vacuole | 0.139 |
| | Lysosomal | 0.133 |
| | Extracellular | 0.108 |
| | ER | 0.083 |
| | Nuclear | 0.082 |
| | Peroxisomal | 0.069 |
| | Golgi | 0.031 |
| | Cytoskeletal | 0.009 |

**********

**Figure 16.** CELLO Result.

---------- Plant-mPLoc Computation Result ----------

| Query protein | Predicted location(s) |
|---|---|
| ADY15026.1 (S)-tetrahydroprotoberberine oxidase [Berberis wilsoniae] | **Cytoplasm.** |

**Figure 17.** Plant-mPloc result

**DISCUSSION**

Berberine is a natural compound with significant pharmacological properties, making it a valuable target in pharmaceutical research. It is present in various plant species, particularly those belonging to the *Berberidaceae, Ranunculaceae*, and *Papaveraceae* families. The compound has garnered attention due to its diverse biological activities, including antimicrobial, anti-inflammatory, and anti-cancer effects. These properties make berberine a promising candidate for the development of therapeutic agents targeting various diseases.

One of the key enzymes involved in the biosynthesis of berberine is (S)-tetrahydroprotoberberine oxidase. This enzyme plays a crucial role in catalyzing a specific step in the biosynthetic pathway leading to the production of berberine. Understanding the structural and functional properties of (S)-

 

tetrahydroprotoberberine oxidase is essential for unraveling its role in berberine biosynthesis and for exploring its potential applications in biotechnology.

By elucidating the structural features of (S)-tetrahydroprotoberberine oxidase, researchers can gain insights into its catalytic mechanism and substrate specificity. Additionally, understanding the enzyme's functional properties, such as its activity and stability, can provide valuable information for biotechnological applications, including the production of berberine and the engineering of microbial hosts for enhanced production.

The research aims to conduct a thorough analysis of the (S)-tetrahydroprotoberberine oxidase enzyme, aiming to understand both its structural and functional aspects. Specific objectives encompass exploring the enzyme's physicochemical properties, such as molecular weight, charge distribution, and stability. Additionally, the study seeks to predict the enzyme's secondary structure and solvent accessibility, providing insights into its overall architecture and potential interactions with other molecules.

Molecular functions and cellular localization will be determined to elucidate the enzyme's role within cellular processes. Furthermore, KEGG pathway analysis will be employed to investigate the enzyme's involvement in metabolic pathways, particularly in berberine biosynthesis and broader plant metabolism. Through these methods, the research aims to shed light on the enzyme's significance in biological processes and its potential applications in biotechnology and drug discovery.

To achieve these objectives, various bioinformatic tools and databases were utilized. The protein sequence of (S)-tetrahydroprotoberberine oxidase was subjected to analysis using tools such as Phobius, Predict Protein, InterProSurf, and KEGG pathway analysis. These analyses provided insights into the enzyme's physicochemical properties, secondary structure, molecular functions, cellular localization, and involvement in metabolic pathways.

Analysis of the enzyme's physicochemical properties revealed crucial information about its composition and characteristics. The enzyme consists of 530 amino acid residues with a molecular weight of 58989.77. The distribution of charged residues indicates a near-neutral charge, with 51 negatively charged and 50 positively charged residues. Additionally, the enzyme exhibits an instability index of 36.41, suggesting potential instability, countered by a high aliphatic index of 89.70, indicating stability under adverse conditions. The hydrophilic nature of the enzyme, reflected in its GRAVY score of -0.059, suggests a propensity to interact with water molecules.

Predictions of the enzyme's secondary structure provided insights into its conformation. The enzyme is predicted to contain alpha helices, beta strands, and other structural elements. The distribution of these secondary structures influences the overall architecture and functional properties of the enzyme.

The enzyme was found to exhibit several molecular functions, including NADPH activity, molybdopterin cofactor binding, molybdenum ion binding, and peroxidase activity. These functions highlight the enzyme's involvement in various biochemical processes, such as redox reactions and cofactor binding, which are crucial for its catalytic activity.

The analysis indicated that the enzyme primarily localizes to the extracellular region and plant-type cell wall. This localization suggests potential roles in extracellular processes, such as cell signaling, defense mechanisms, or structural support within the cell wall.

The enzyme is implicated in several KEGG pathways, including the biosynthesis of secondary metabolites, metabolic pathways, nitrogen metabolism, and phenylpropanoid biosynthesis. These

 

pathways underscore the enzyme's involvement in diverse metabolic processes, particularly secondary metabolite biosynthesis and nitrogen utilization. Using the Phobius tool, it was observed that the enzyme is located outside the cell, indicating a non-cytoplasmic localization. This finding further supports the enzyme's potential roles in extracellular processes or interactions with external molecules.

The configuration and placement of transmembrane helices or domains within the enzyme's structure were analyzed using the Phobius server. This analysis helps in understanding the enzyme's orientation within the cell membrane, which is crucial for its function and interactions with other cellular components.

The ProFunc server was employed to identify potential functional roles of the enzyme based on its three-dimensional structure. This analysis provides insights into the enzyme's functional annotation, aiding in understanding its role in biological processes and potential therapeutic applications. The InterProSurf tool was utilized to analyze the enzyme's surface properties, including solvent accessibility, hydrophobicity, electrostatic potential, and regions likely to be involved in protein-protein interactions or ligand binding. This analysis provides information on the enzyme's surface characteristics and potential functional implications.

The predict protein software was used to predict structural features, evolutionary stability, and functional interactions of the enzyme. This analysis provided important insights into the enzyme's secondary structure, solvent accessibility, sequence length, and potential homologous proteins.

SOPMA analysis predicted the secondary structure elements of the enzyme, including alpha helices, beta strands, coils, and turns. Understanding the enzyme's secondary structure is crucial for elucidating its overall architecture and functional properties. These results provide a comprehensive understanding of the (S)-tetrahydroprotoberberine oxidase enzyme, elucidating its structural features, functional properties, cellular localization, and involvement in metabolic pathways. Such insights are crucial for unraveling the enzyme's biological significance, potential applications in biotechnology, and role in berberine biosynthesis.

## CONCLUSION

This research has provided valuable insights into the structural and functional characteristics of the (S)-tetrahydroprotoberberine oxidase enzyme, shedding light on its role in berberine biosynthesis and potential applications in biotechnology and pharmaceutical research. The analysis of physicochemical properties, secondary structure, molecular functions, and cellular localization has revealed important features of the enzyme, contributing to our understanding of its biochemical properties. Furthermore, KEGG pathway analysis has highlighted the enzyme's involvement in metabolic pathways relevant to berberine biosynthesis and plant metabolism.

The major findings of this study include the prediction of the enzyme's secondary structure, solvent accessibility, and transmembrane topology, which provide insights into its structural organization and potential functional implications. Additionally, the identification of functional annotations and protein-protein interaction sites has enhanced our understanding of the enzyme's biological roles. Moreover, the analysis of surface properties and evolutionary stability has provided further insights into the enzyme's structural and functional properties.

However, it is essential to acknowledge the limitations of this study. The predictions and analyses performed in silico are based on computational algorithms and may have inherent limitations and inaccuracies. Experimental validation of the predicted findings is necessary to confirm the enzyme's structural and functional properties. Additionally, the scope of this study is limited to bioinformatics analysis, and further biochemical and biophysical studies are required to fully characterize the (S)-tetrahydroprotoberberine oxidase enzyme. In summary, despite its limitations, this research has contributed to our understanding of the (S)-tetrahydroprotoberberine oxidase enzyme and provided a

 

foundation for future studies aimed at exploring its biochemical properties and biotechnological applications.

**Acknowledgement**

The authors thank BioNome (http://bionome.in) for providing us with the necessary computational facilities and research support for conducting this research.

## Abbreviations

| S.N. | Abbreviation | Description |
|---|---|---|
| 1. | BBR | Berberine |
| 2. | BBE | Berberine Bridge Enzyme |
| 3. | CNS | Central Nervous System |
| 4. | FAD | Flavin Adenine Dinucleotide |
| 5. | GRAVY | Grand Average of Hydropathicity |
| 6. | GMQE | Global Model Quality Estimation |
| 7. | KF | Kaempferol |
| 8. | NCBI | NatioCenter for Biotechnology Information |
| 9. | PAH | Phenylalanine Hydroxylase |
| 10. | PDB | Protein Data Bank |
| 11. | PPI | Protein-Protein Interaction |
| 12. | STRING | Search Tool for the Retrieval of Interacting Genes/Proteins |
| 13. | SOPMA | Self-Optimized Prediction Method with Alignment |
| 14. | STOX | (S)-tetrahydroprotoberberine oxidase |
| 15. | THPB | Tetrahydroprotoberberine |

## REFERENCES

1. Adejoke HT, Louis H, Amusan OO, Apebende G. A review on classes, extraction, purification and pharmaceutical importance of plants alkaloid. J Med Chem Sci. 2019;2:130–139.
2. Ali F, Alom S, Zaman MK. Berberine: a comprehensive review on its isolation, biosynthesis, chemistry and pharmacology. Asian J Chem. 2021;33(11):2548–2560. doi:10.14233/ajchem.2021.23365.
3. Amann M, Nagakura N, Zenk MH. Purification and properties of (S)-tetrahydroprotoberberine oxidase from suspension-cultured cells of Berberis wilsoniae. 1988;175(1):17–25. doi:10.1111/j.1432-1033.1988.tb14160.x.
4. Cheng Z, Kang C, Che S, SU J, Sun Q, Ge T, Guo Y, Lv J, Sun Z, Yang W, Li X, Cui R. Berberine: a promising treatment for neurodegenerative diseases. Front Pharmacol. 2022;13:845591. doi:10.3389/fphar.2022.845591.
5. Debnath B, Singh WS, Das M, Goswami S, Singh MK, Maiti D, Manna K. Role of plant alkaloids on human health: a review of biological activities. Mater Today Chem. 2018;9:56–72. doi:10.1016/j.mtchem.2018.05.001.
6. Deng X, Zhao I, Fang T, Xiong Y, Ogutu C, Yang D, Vimolmangkang S, Liu Y, Han Y. Investigation of benzylisoquinoline alkaloid biosynthetic pathway and its transcriptional regulation in lotus. 2018;5:29. doi:10.1038/s41438-018-0035-0.
7. Dey P, Kundu A, Kumar A, Gupta M, Lee BM, Bhakta T, Dash S, Kim HS. Analysis of alkaloids (indole alkaloids, isoquinoline alkaloids, tropane alkaloids). Recent Advances in Natural Products Analysis. Amsterdam, Netherlands: Elsevier; 2020. 505–567. doi:10.1016/B978-0-12-816455-6.00015-9.
8. Dincheva I, Badjakov I, Galunska B. New insights into the research of bioactive compounds from

 

plant origins with nutraceutical and pharmaceutical potential. Plants. 2023;12(2):258. doi:10.3390/plants12020258.
9. Heinrich M, Mah J, Amirkia V. Alkaloids used as medicines: structural phytochemistry meets biodiversity - an update and forward look. Mol. 2021;26(7):1836. doi:10.3390/molecules26071836.
10. Jamshidi-Kia F, Lorigooini Z, Amini-Khoei H. Medicinal plants: past history and future perspective. J Herbmed Pharmacol. 2018;7(1):1–7. doi:10.15171/jhp.2018.01.
11. Majolo F, Delwing LKDOB, Marmitt DJ, Bustamante-Filho IC, Goettert MI. Medicinal plants and bioactive natural compounds for cancer treatment: important advances for drug discovery. Phytochem Lett. 2019;31:196–207. doi:10.1016/j.phytol.2019.04.003.0.
12. Martirosyan D, Miller E. Bioactive compounds: the key to functional foods. Bioact Compd Health Dis. 2018;1(3):36–39. doi:10.31989/bchd.v1i3.539.
13. Mbuni YM, Wang S, Mwangi BN, Mbari NJ, Musili PM, Walter NO, Hu G, Zhou Y, Wang Q. Medicinal plants and their traditional uses in local communities around Cherangani hills, Western Kenya. Plants. 2020;9(3):331. doi:10.3390/plants9030331.
14. Mujtaba MA, Akhter MH, Ali MS, Hussain DM. An updated review on therapeutic potential and recent advances in drug delivery of berberine: current status and future prospect. Curr Pharm Biotechnol. 2022;23(1):60–71. doi:10.2174/1389201022666210208152113.
15. Nasim N, Sandeep IS, Mohanty S. Plant-derived natural products for drug discovery: current approaches and prospects. Nucleus. 2022;65(3):399–411. doi:10.1007/s13237-022-00405-3.
16. Pandaressh MD, Mythri RB, Bharath MMS. Bioavailability of dietary polyphenols: factors contributing to their clinical application in CNS diseases. Neurochem Int. 2015;89:198–208. doi:10.1016/j.neuint.2015.07.003.
17. Pereira AG, Cassani L, Garcia-Oliveira P, Otero P, Mansoor S, Echave J, Xiao J, Simal-Gandara J, Prieto MA. Plant Alkaloids: Production, Extraction, and Potential Therapeutic Properties. In: Carocho M, Heleno SA, Barros L, editors. Natural Secondary Metabolites. Cham, Switzerland: Springer; 2023. 157–200. doi:10.1007/978-3-031-18587-8_6.
18. Prajwala B, Raghu N, Gopenath TS, Kaginelli SB, Karthikeyan M, Ashok G, Ranjith MS, Srinivasan V, Basalingappa KM. Berberine and its pharmacology potential: a review. Eur J Biomed Pharm Sci. 2020;7(5):115–123.
19. Salmeron-Manzano E, Garrido-Cardenas JA, Manzano-Agugliaro F. Worldwide research trends on medicinal plants. Int J Environ Res Public Health. 2020;17(10):3376. doi:10.3390/ijerph17103376.
20. Santhan P. A field study on Indian medicinal plants. J Med Plants Stud. 2020;8(4):198–205.
21. Santos JSD, Cirino JPG, Carvalho PDO, Ortega MM. The pharmacological action of kaemferol in central nervous system diseases: a review. Front Pharmacol. 2020;11:565700. doi:10.3389/fphar.2020.565700.
22. Shakya AK. Medicinal plants: future source of new drugs. Int J Herb Med. 2016;4(4):59–64.
23. Sobhani Z, Akaberi M, Amiri MS, Ramezani M, Emami SA, Sahebkar A. Medicinal Species of the Genus Berberis: A review of Their Traditional and Ethnomedicinal Uses, Phytochemistry and Pharmacology. In: Barreto GE, Sahebkar A, editors. Pharmacological Properties of Plant-Derived Natural Products and Implications for Human Health. Advances in Experimental Medicine and Biology. Cham: Springer; 2021. 547–577. doi:10.1007/978-3-030-64872-5_27.
24. Yudharaj P, Shankar M, Sowjanya R, Sireesha B, Naik EA, Priyadarshini RJ. Importance and uses of medicinal plants – an overview. Int J Preclin Pharm Res. 2016;7(2):67–73.

 